\



Plasma assisted molecular beam epitaxial growth of GaN with low growth rates and their properties

Zhen-Hua Li(李振华), Peng-Fei Shao(邵鹏飞), Gen-Jun Shi(施根俊), Yao-Zheng Wu(吴耀政), Zheng-Peng Wang(汪正鹏), Si-Qi Li(李思琦), Dong-Qi Zhang(张东祺), Tao Tao(陶涛), Qing-Jun Xu(徐庆君), Zi-Li Xie(谢自力), Jian-Dong Ye(叶建东), Dun-Jun Chen(陈敦军), Bin Liu(刘斌), Ke Wang(王科), You-Dou Zheng(郑有炓), and Rong Zhang(张荣)

Citation: Chin. Phys. B, 2022, 31 (**1**): 018102. DOI: 10.1088/1674-1056/ac339d
Journal homepage: http://cpb.iphy.ac.cn; http://iopscience.iop.org/cpb

What follows is a list of articles you may be interested in

Removal of GaN film over AlGaN with inductively coupled BCl_3/Ar atomic layer etch

Jia-Le Tang(唐家乐) and Chao Liu(刘超)
Chin. Phys. B, 2022, 31 (**1**): 018101. DOI: 10.1088/1674-1056/ac032d

Vertical MBE growth of Si fins on sub-10 nm patterned substrate for high-performance FinFET technology

Shuang Sun(孙爽), Jian-Huan Wang(王建桓), Bao-Tong Zhang(张宝通), Xiao-Kang Li(李小康), Qi-Feng Cai(蔡其峰), Xia An(安霞), Xiao-Yan Xu(许晓燕), Jian-Jun Zhang(张建军), and Ming Li(黎明)
Chin. Phys. B, 2021, 30 (**7**): 078104. DOI: 10.1088/1674-1056/abf63f

Growth of high-crystallinity uniform GaAs nanowire arrays by molecular beam epitaxy

Yu-Bin Kang(亢玉彬), Feng-Yuan Lin(林逢源), Ke-Xue Li(李科学), Ji-Long Tang(唐吉龙), Xiao-Bing Hou(侯效兵), Deng-Kui Wang(王登魁), Xuan Fang(方铉), Dan Fang(房丹), Xin-Wei Wang(王新伟), and Zhi-Peng Wei(魏志鹏)
Chin. Phys. B, 2021, 30 (**7**): 078102. DOI: 10.1088/1674-1056/abf920

Epitaxial growth and air-stability of monolayer Cu_2Te

K Qian(钱凯), L Gao(高蕾), H Li(李航), S Zhang(张帅), J H Yan(严佳浩), C Liu(刘晨), J O Wang(王嘉鸥), T Qian(钱天), H Ding(丁洪), Y Y Zhang(张余洋), X Lin(林晓), S X Du(杜世萱), H-J Gao(高鸿钧)
Chin. Phys. B, 2020, 29 (**1**): 018104. DOI: 10.1088/1674-1056/ab5781

A review on MBE-grown HgCdSe infrared materials on GaSb (211)B substrates

Z K Zhang, W W Pan, J L Liu, W Lei
Chin. Phys. B, 2019, 28 (**1**): 018103. DOI: 10.1088/1674-1056/28/1/018103

Plasma assisted molecular beam epitaxial growth of GaN with low growth rates and their properties

Zhen-Hua Li(李振华)[1,2], Peng-Fei Shao(邵鹏飞)[1], Gen-Jun Shi(施根俊)[1], Yao-Zheng Wu(吴耀政)[1], Zheng-Peng Wang(汪正鹏)[1], Si-Qi Li(李思琦)[1], Dong-Qi Zhang(张东祺)[1], Tao Tao(陶涛)[1], Qing-Jun Xu(徐庆君)[3], Zi-Li Xie(谢自力)[1], Jian-Dong Ye(叶建东)[1], Dun-Jun Chen(陈敦军)[1], Bin Liu(刘斌)[1,†], Ke Wang(王科)[1,‡], You-Dou Zheng(郑有炓)[1], and Rong Zhang(张荣)[1,4]

[1] *Jiangsu Provincial Key Laboratory of Advanced Photonic and Electronic Materials, School of Electronic Science and Engineering, Nanjing University, Nanjing, China*

[2] *College of Optoelectronics Engineering, Zaozhuang University, Zaozhuang* 277160, *China*

[3] *Institute of Novel Semiconductors, State Key Laboratory of Crystal Material, Shandong University, Jinan* 250100, *China*

[4] *Xiamen University, Xiamen* 361005, *China*

(Received 23 August 2021; revised manuscript received 18 October 2021; accepted manuscript online 27 October 2021)

A systematic investigation on PA-MBE grown GaN with low growth rates (less than 0.2 μm/h) has been conducted in a wide growth temperature range, in order to guide future growth of sophisticated fine structures for quantum device applications. Similar to usual growths with higher growth rates, three growth regions have been revealed, namely, Ga droplets, slightly Ga-rich and N-rich 3D growth regions. The slightly Ga-rich region is preferred, in which GaN epilayers demonstrate optimal crystalline quality, which has been demonstrated by streaky RHEED patterns, atomic smooth surface morphology, and very low defect related yellow and blue luminescence bands. The growth temperature is a critical parameter to obtain high quality materials and the optimal growth temperature window (∼ 700–760 °C) has been identified. The growth rate shows a strong dependence on growth temperatures in the optimal temperature window, and attention must be paid when growing fine structures at a low growth rate. Mg and Si doped GaN were also studied, and both p- and n-type materials were obtained.

Keywords: GaN, molecular beam epitaxy (MBE), low growth rate, growth diagram

PACS: 81.05.Ea, 81.10.–h, 81.15.Hi **DOI:** 10.1088/1674-1056/ac339d

1. Introduction

Group III-nitride semiconductors with their wide applications in light emitting diodes and electronic devices have attracted much interest. GaN is the basic material of the group III-nitride materials family.[1–3] Although metal organic chemical vapor deposition (MOCVD) is overwhelming in the III-nitride device markets, plasma assisted molecular beam epitaxy (PA-MBE) is another important epitaxy technique to grow III nitride materials and devices.[4–11] Compared to MOCVD, MBE has some advantages, such as an ultrahigh vacuum and ultra-clean environment for growth with low impurity levels, precise control of epilayer thickness, atomic level sharp interfaces, hydrogen free environment for automatic activation of Mg acceptors, and high indium content alloys at relatively low temperatures. Especially, MBE is suitable for growing devices with sophisticated fine structures and quantum effect structures, thanks to its much faster source supply switch ability.[12–15] Many research groups have investigated PA-MBE III nitrides from fundamental physics and material growth mechanism, to its potential for sophisticated devices. PA-MBE GaN growth diagrams have been well established as an instruction to find optimal growth conditions.[16,17]

In fact, a high MBE growth rate for III nitride has been seek for a long time to explore MBE's potential for mass production. A growth rate of 10 μm/h has been achieved recently based on a specially MBE system with extremely high pumping ability.[18,19] Majority studies have focused on a range varying from ∼ 0.3 μm/h to 1–3 μm/h.[15,20,21] However, a low growth rate is necessary for better control on epilayer thickness and interface sharpness in some cases, such as resonant tunneling diodes, intersubband devices based on multiple quantum wells, and superlattices. In this work, we focus on the rarely studied low growth rate range, less than 0.3 μm/h, intended to guide for future growths of sophisticated fine structures.

2. Experiments

All GaN layers were grown on *c*-plane hydride vapor phase epitaxy grown GaN/sapphire templates in a RIBER Compact T-21 PA-MBE system. The MBE system is equipped with five metal Knudsen cells (two Ga cells, two Al cells, and one In cell), two doping cells (Mg, Si), and one radio frequency nitrogen plasma cell. Reflective high energy diffrac-

†Corresponding author. E-mail: bliu@nju.edu.cn

‡Corresponding author. E-mail: kewang@nju.edu.cn

© 2022 Chinese Physical Society and IOP Publishing Ltd

tion (RHEED) was used to monitor the growth process *in situ*. The growth temperature was measured by both thermocouple and pyrometer. All growth temperatures here are the calibrated pyrometer temperatures. A 1-μm-thick titanium layer was deposited on the backsides of the templates as a heat absorption backcoating.

Nine series of GaN epilayers were grown by PA-MBE in a wide temperature range from 580 °C to 790 °C under various nitrogen plasma conditions to study growth rates, growth mechanism, surface morphology, luminescence properties, doping, etc. Series 1 and 2 were grown to investigate GaN growth rates at low and high growth temperatures. Nitrogen gas flow rates varied from 0.7 sccm to 1.3 sccm and radio frequency power varied from 400 W to 550 W. To study the PA-MBE GaN growth mechanism and determine boundaries between growth regions, series 3–7 were grown with the nitrogen gas flow and RF-power kept at 0.7 sccm and 450 W, respectively. The series 3 were grown at the low temperature range (580–630 °C) in which the Ga flux varied from 3.8×10^{-7} Torr to 4.8×10^{-7} Torr. Series 4 and 5 were grown at the mediate temperature range (685–725 °C) in which the Ga flux varied from 2.0×10^{-7} Torr to 3.2×10^{-6} Torr. Series 6 and 7 were grown at the high temperature range (760–790 °C) in which the Ga flux varied from 9.9×10^{-7} Torr to 9.9×10^{-6} Torr. Mg doped GaN and Si doped GaN were both grown which are marked as series 8 and 9, respectively. After growth, the surface morphology of the GaN epilayers was characterized by using atomic force microscope (AFM). Optical properties of the GaN epilayers were studied by the room temperature photoluminescence (PL) spectra with a 325 nm laser as the excitation light sources. The thicknesses of the GaN epilayers were measured by the scanning electron microscope (SEM). Additionally, the dopant concentration depth profile and electrical properties of the doped GaN were studied by second ion mass spectroscopy (SIMS) and Hall effect measurement.

3. Results and discussion

3.1. Growth rates under various nitrogen plasma conditions

Series 1 and 2 were grown at 615 °C and 760 °C, respectively, and their growth rates, together with more data points at the various growth temperatures, are shown in Fig. 1. The corresponding growth regions, namely, Ga droplets, slightly Ga-rich and 3-dimension (3D) growth (N-rich) regions, are indicated by different symbols. Detailed analysis of the growth regions will be discussed in the next section. The amount of active nitrogen species is mainly determined by the nitrogen gas flow rate and RF-power.[22] For the samples grown at 615 °C in the Ga droplets region or 760 °C in the slightly Ga-rich region, the growth rate increases as the nitrogen flow rate and RF-power increase as shown by the dashed lines guide for eyes, demonstrating the fact that the growth rate is limited by the amount of active nitrogen for the Ga-rich regions (slightly Ga-rich and Ga droplets).

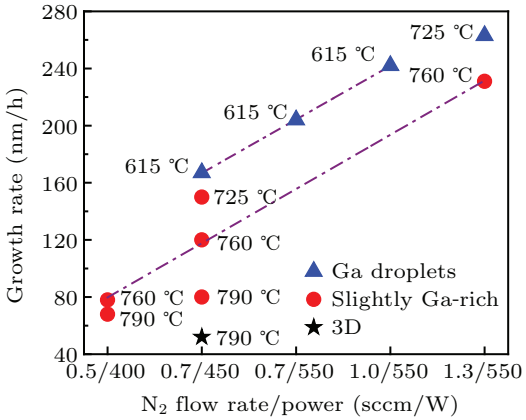


Fig. 1. Growth rates of the GaN epilayers grown by PA-MBE as the plasma condition varies. The dash lines are only guide for eyes for 615 °C and 760 °C respectively.

When the plasma conditions are constant as 0.7 sccm and 450 W, the growth rate shows a severe decrease, from 166 nm/h down to 80 nm/h, as the growth temperature increases from 615 °C to 790 °C in the Ga-rich region. When the temperature increases to 725 °C, the growth rate slightly decreases to 154 nm/h, but the decrease accelerates when the temperature increases to 760 °C and 790 °C. This is a striking contrast to the literature reports which studied MBE grown GaN at much higher growth rates. Van Mil *et al.* reported almost no growth rate drop up to 810 °C[23] with an initial growth rate of around 300 nm/h. This difference is attributed to the exponential increase of GaN decomposition in the high temperature range,[23,24] competing with the limited growth rate in our work. Consequently, special attention must be paid to the sensitive dependence on the growth temperature when growing fine structures at a low growth rate. For the 3D region, since the Ga supply is extremely lower than the active nitrogen and it is not enough to consume all active nitrogen adatoms on the growth front, the GaN growth rate is further decreased down to 50 nm/h.

3.2. Surface morphology, *in situ* RHEED patterns, and growth diagram of PA-MBE GaN epilayers

Based on the above experimental results, the nitrogen plasma conditions were fixed at a nitrogen flow rate of 0.7 sccm and RF-power of 450 W, and series 3–7 were grown with various Ga fluxes at temperatures from 580 °C to 790 °C. A detailed experimental investigation on the growth mechanism and layer properties was conducted in this low growth rate range.

Figures 2 and 3 show surface morphology evolution and roughness root mean square (RMS) variation of GaN epilayers

as the growth temperature varies. Figure 4 shows the evolution of RHEED patterns during growth as the Ga flux decreases. The three growth regions and the corresponding surface morphology characterization are determined, which is similar to the well established three growth regions at the usual higher growth rates.

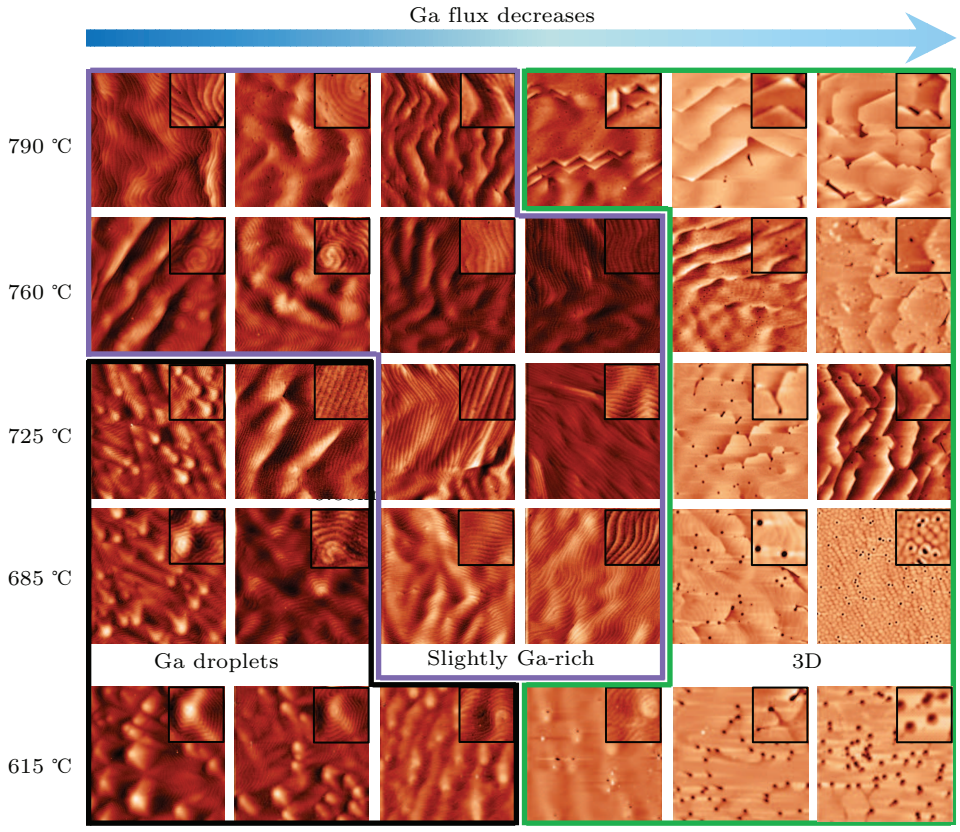


Fig. 2. The 5×5 μm^2 AFM images (inset: 1×1 μm^2) of the surface morphology evolution as the growth temperatures and growth regions vary for the GaN epilayers grown by PA-MBE. The nitrogen gas flow is 0.7 sccm and RF-power is 450 W.

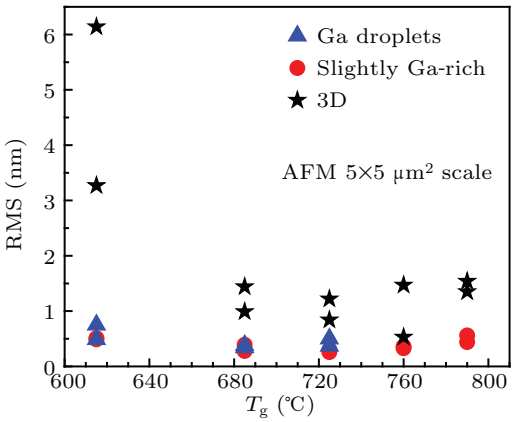


Fig. 3. The surface roughness RMS values (5×5 μm^2) of the GaN epilayers grown by PA-MBE varies at different growth temperature for the three growth regions. The nitrogen gas flow is 0.7 sccm and RF-power is 450 W.

In the Ga droplets region, RHEED patterns are dim and streaky due to relatively smooth crystal surface but on which excess Ga droplets form, lowering the brightness. When taken out from the MBE chamber and checked under an optical microscope, Ga metal droplets were observed (not shown here and etched by HCl before AFM experiments). In fact, the shadow effect of the Ga droplets on surface results in the dim RHEED intensity. Many spiral hillocks surrounded by stepped terraces are observed, for instance, 615 °C (left two AFM images) and 725 °C (the first left AFM image). The height of the stepped terraces is ∼ 0.2–0.3 nm, which agrees well with one (001) GaN monolayer. Each spiral hillock shaped structure consists of two interlocking spiral ramps correlated to the mixed type dislocation.[25] The surface RMS roughness is around 0.3–0.8 nm in this region, as shown by blue-triangles in Fig. 3.

In the slightly Ga-rich region, RHEED patterns are also streaky and slightly brighter than Ga droplet cases, but still quite dim, which is expected and due to coverage of the Ga adlayer consisting of about two monolayers of Ga adatoms.[17,22,26,27] Clear step flow growth mode has been revealed by the AFM images, for example, showing in the 2nd, 3rd and 4th AFM images from left for 725 °C. Atomically smooth surfaces have been obtained via the step flow growth mode in this growth region. The surface RMS roughness is about 0.2–0.4 nm for most cases in this region, only except at extremely high temperature (RMS ∼ 0.5 nm at 790 °C). As the temperature increases, this slightly Ga-rich growth region covers a wider Ga flux range and shifts to much higher Ga flux values. The step flow growth is attributed to increased adatom surface mobilities via the Ga wetting layer, an extra diffusion channel, under Ga-rich conditions.[20,28]

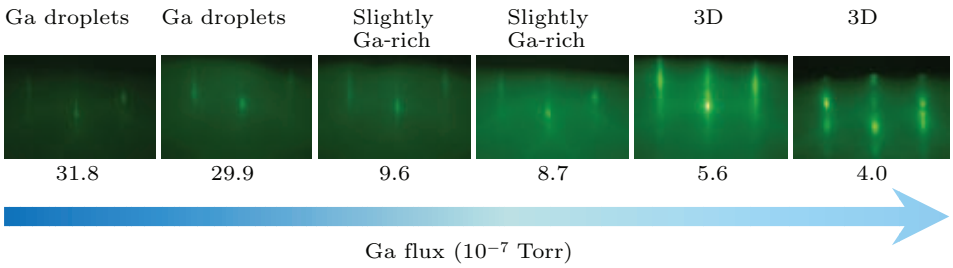


Fig. 4. Typical evolution of RHEED patterns along the direction [11$\bar{2}$0] for the GaN epilayers grown at 718 °C. The nitrogen gas flow is 0.7 sccm and RF-power is 450 W. The blue arrow shows that the growth region gradually changes from Ga droplets to 3D as the Ga flux decreases.

In the 3D region (N-rich condition), RHEED patterns are bright and spotty due to the surface asperity, indicating 3D island growth mode. Many pits and trenches appear on the AFM images. The RMS roughness is the highest in the low temperature range. And incomplete coalescence and grainy structures appear, for instance, the 1st AFM image from right hand side for both 615 °C and 685 °C, resulting in trenches and grain boundaries and very rough surfaces. As temperature increases (685 °C to 790 °C), however, hexagonal coalesced two-dimensional-platelet-like structures have been observed and step-bunching happens. The height of the step-bunching is $\sim$ 3.0–6.0 nm. The surface morphology is characterized by atomically flat hexagonal platelets which are separated by pits, trenches and steps, resulting in average RMS roughness around 1.0–1.5 nm. At the extremely high temperature, several-micro-meter size hexagonal platelets can be seen, for example, right two AFM images for 790 °C, which indicates very high decomposition competing with growth and is consistent with the drastically decreased growth rate in Fig. 1. If increasing Ga fluxes, the 2D platelets gradually coalesce, revealing the evolution towards intermediate growth (slightly Ga-rich). The dark pits appear almost in all samples grown in the 3D growth region and their density is 2×10^8–4×10^8 cm^{-2}, which is a typical value for MOCVD GaN dislocation density, suggesting that the pits originate from threading dislocations on the GaN templates.[21]

Based on the characterization results of series 3–7 samples, the PA-MBE growth diagram was summarized. In the growth diagram, there are three main growth regions identified: Ga droplets, slightly Ga-rich, and 3-dimension (3D), as shown in Fig. 5. The boundaries of the growth regions are indicated by the dotted lines, which are identified based on the results of RHEED patterns and surface morphologies. At a fixed growth temperature, if it is high enough (> 640 °C), the growth changes from 3D to slightly Ga-rich, and then to Ga droplets as the Ga flux increases; while at a lower temperature (< 640 °C), directly from 3D to Ga droplet region. The Ga/N ratio and growth temperature basically determine the growth kinetics, and thus the growth region, the RHEED patterns and surface morphologies, as discussed above.

In the 3D region (N-rich), the GaN growth rate is limited by the available Ga flux since all excess N desorbs from the surface. The lack of Ga supply and absence of Ga wetting layers cause low diffusion mobilities for both Ga and N adatoms, resulting in spotty RHEED and a rough surface morphology with a lot of pits, where the dislocation terminals are located. In contrast, for Ga-rich growth the available N flux limits the growth rate but excess Ga can accumulate on the surface depending strongly on the amount of supplied Ga flux and the growth temperature. This leads to two Ga-rich regions, slightly Ga-rich and Ga droplets. Slightly Ga rich (intermediate) region is characterized by a Ga wetting layer, which is well known and consists of $\sim$ 2 monolayers of Ga adatom coverage. The Ga bilayers behave like a liquid metallic film with weak metallic Ga–Ga bond, offering a diffusion channel for arrived N atoms and enhancing their surface migration.[20,28–31] The impinging N adatoms consequently diffuse to a preferable incorporation site, consuming the liquid-like Ga atoms, and the impinging Ga atoms maintain the Ga bilayers coverage, resulting in the observed atomic smooth step flow morphology. The Ga-droplet region is characterized by the Ga bilayers plus accumulated Ga droplets on the top, which are Ga reservoirs to supply Ga atoms to maintain the underlaying Ga bilayers during the GaN growth. The spiral hillocks are supposed to be generated from the excess Ga adatoms accumulation where the screw dislocation propagates along the *c*-axis direction.[32,33]

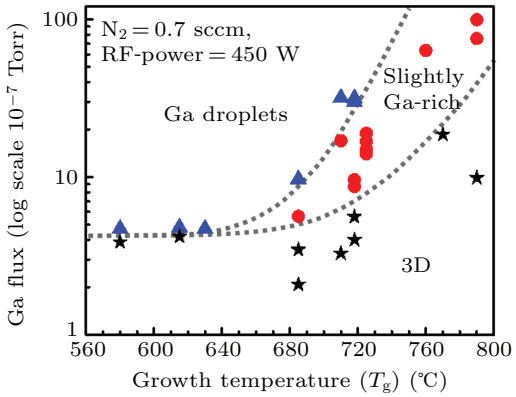


Fig. 5. The growth diagram with the three regions: Ga dorplets, slightly Ga-rich, and 3D for the GaN epilayers grown by PA-MBE.

As one can see in Fig. 5, as the growth temperature increases, the Ga flux boundaries between growth regions shift to higher Ga flux, and the window of Ga flux for the slightly Ga-rich region becomes wider, which is the preferred growth

condition for optimal crystalline quality. This is attributed to the combined effect of the stability of the Ga bilayer coverage, which can be maintained at the growth front at temperatures above $\sim$ 640 °C, and the exponentially increased Ga adatom desorption rate as the growth temperatures elevates.

In the temperature range below $\sim$ 640 °C, the Ga desorption rate is almost negligible and Ga mobility is also low. Consequently, Ga droplets form once the supplied Ga/N is above the stoichiometric condition, and no Ga flux window can maintain the Ga adlayers only. In the temperature range $>$ 640 °C, the window of Ga flux for the slightly Ga-rich region becomes wider and wider since the Ga desorption rate become higher as the temperature increases. It becomes easy to achieve this growth region. When the temperature is very high, $>\sim$ 760 °C, the Ga desorption rate becomes much higher so that a very high Ga flux is necessary to maintain the Ga adlayer coverage and an extremely high Ga flux is required to reach Ga droplets region (not reached in this report). However, elevating the temperature further leads to strong GaN decomposition competing with growth, which consequently results in much reduced growth rates.

Compared with the growth diagram reported by Koblmüller *et al.*,[17] no 2D layer by layer growth mode has been observed in our experiments and the Ga flux required to maintain the Ga adlayer (two monolayers) coverage in the growth font is obviously higher than the usual cases for low growth rates of GaN in this work. In Ref. [17], the 2D layer by layer growth mode is the transition between the 3D and step flow growth mode at higher growth rates (constant N flux of 4.8 nm/min), which is characterized by clear RHEED intensity oscillation and happens at a condition close to N-rich conditions. This difference is probably due to the much lower growth rate of GaN in our study, which is caused by the smaller amount of the active nitrogen. In such case, the window for layer by layer growth mode is perhaps very narrow.

3.3. Optical properties

Figure 6(a) shows the room temperature PL spectra for GaN in the three growth regions and the yellow luminescence band (YL) and near band edge (NBE) peaks are at around 2.25 eV and 3.43 eV, respectively. In the 3D growth regions, the blue luminescence band (BL) is also observed at around 2.7–3.0 eV. The yellow band is attributed to gallium vacancies (V_{Ga}), V_{Ga} related complex, or carbon impurities.[34,35] The blue band is caused by the transitions from shallow donors or conduction band to a deep acceptor and attributed to the V_{Ga} related complex or some impurities.[34,36–38] Compared with the GaN in Ga-rich growth region, the GaN in 3D growth region, namely, N-rich condition, may have higher density of V_{Ga} or V_{Ga} related complex, which causes the higher intensity of the yellow band and the appearance of the blue band. Figure 6(b) shows the YL and NBE integrated intensity ratio for GaN in the three growth regions. The smaller ratio is obtained for GaN in the Ga-rich growth region. Thus, it indicates that the most suitable growth region for growing GaN is slightly Ga-rich. Figure 6(c) shows

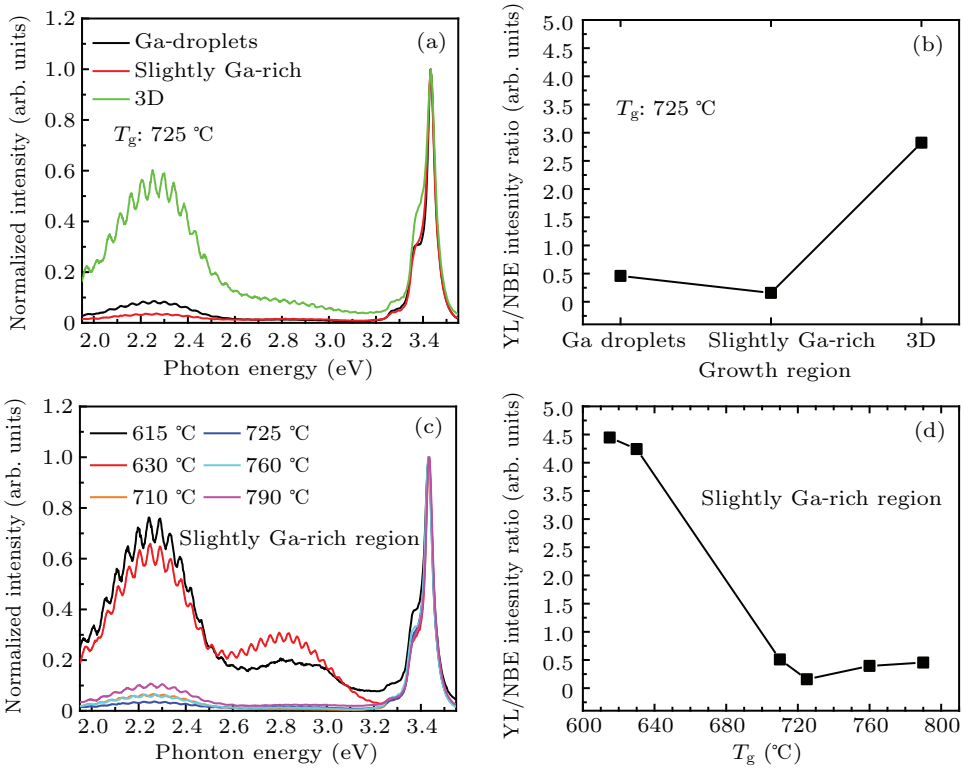


Fig. 6. (a) Room temperature PL spectra, and (b) the YL and NBE integrated intensity ratio for GaN in PL spectra for the three growth regions; (c) room temperature PL spectra and (d) the ratio of integrated intensity of YL and NBE for GaN in PL spectra with different growth temperatures.

the room temperature PL spectra as the growth temperatures vary, all in the slightly Ga-rich region. For the lower growth temperature, for example below 630 °C, the blue band is also observed. The intensity of the blue band decreases as the growth temperature increases and finally disappears beyond 710 °C. At the lower growth temperature, GaN epilayers may involve relatively high density of impurities and mis-fit dislocations, which cause the intense blue and yellow bands. Figure 6(d) shows the YL and NBE integrated intensity ratio for GaN at different temperatures, and the ratio for GaN grown at a low growth temperature is much higher than that of GaN grown at a high growth temperature. It indicates that the crystal quality of GaN becomes higher at the high growth temperature.

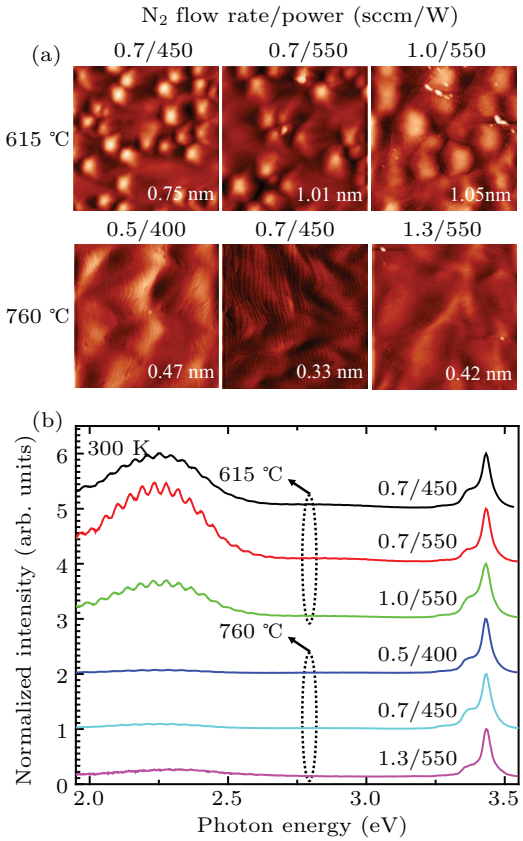


Fig. 7. (a) The AFM images (5×5 μm^2) with the RSM values and (b) room temperature PL spectra for the GaN epilayers grown at 615 °C and 760 °C with the different growth rates.

Figure 7 shows the surface morphology and the optical characterization for the different plasma conditions. At the low temperature 615 °C, the growth process is easy to be in the Ga droplets region which has been discussed above. All the surface morphologies of the three GaN epilayers for the different plasma conditions appear typically hillocks with steps and the average surface roughness is about 0.94 nm. Their PL spectra show that the intensity of the yellow band is very high and the FWHM of the NBE peak is almost similar as about 45 meV. In contrast, at the higher growth temperature 760 °C, the surface morphologies of three GaN epilayers for the different plasma conditions appear typically step flows and the average surface roughness is about 0.41 nm. Their PL spectra show that the intensity of the yellow band is low and the FWHM of the NBE peak is similar as about 35 meV. Therefore, increasing the growth temperature is able to improve the surface morphology and crystal quality of the GaN epilayers which is in consistent with the above discussion. It also indicates that the growth rate has slight influences on the surface morphology and crystal quality of the GaN epilayers, compared with the growth temperature.

3.4. Mg and Si doped GaN epilayers grown by PA-MBE

Since the optimized growth temperature window was obtained under plasma conditions of 0.7 sccm/450 W, the Mg and Si doped GaN epilayers were grown in slightly Ga-rich region indexed as series 8 and 9 respectively, in order to obtain n- and p-type GaN.

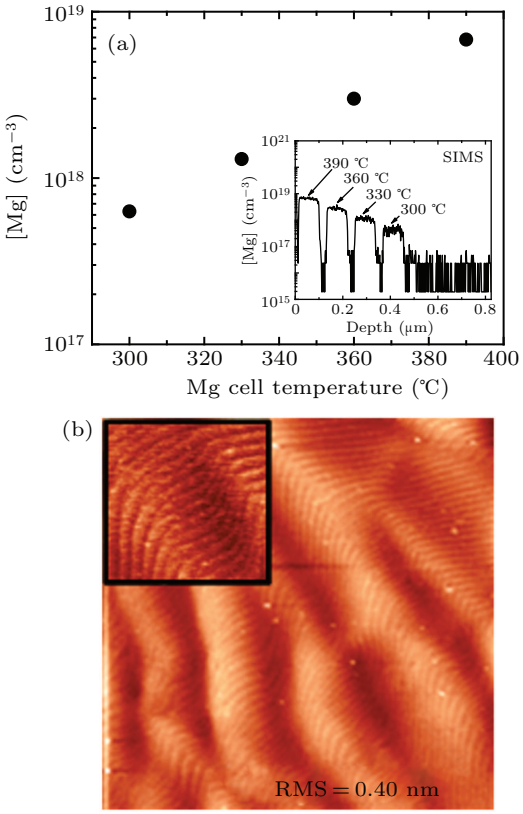


Fig. 8. (a) Mg concentration with various Mg cell temperatures (the inset is Mg concentration depth profile measured by SIMS in step Mg doped GaN epilayer grown with various Mg cell temperatures). (b) AFM images, 5×5 μm^2 (inset: 2×2 μm^2), of a separate Mg doped GaN epilayer with a Mg cell temperature of 390 °C.

To determine dopant concentration as a function of cell temperature, a Mg concentration stepped structure was grown at four Mg cell temperatures, separated by undoped GaN, on an unintentionally doped GaN template. Figure 8(a) shows Mg concentration with four steps of various Mg cell temperatures from 300 °C to 390 °C which was measured by secondary ion mass spectroscopy (SIMS). The Mg concentration

increases as the Mg cell temperature increases from 300 °C to 390 °C. The Mg concentration of 6.8×10^{18} cm^{-3} is obtained at 390 °C. Two additional GaN:Mg samples (Mg cell at 360 °C and 390 °C) were grown on semi-insulating (carbon doped) GaN templates for the Hall effect measurement at room temperature. The 390 °C Mg doped GaN epilayer shows P type conduction with a hole concentration of 3.0×10^{17} cm^{-3}. A smooth surface with clear atomic steps is shown in Fig. 8(b).

The red squares in Fig. 9 are the measured SIMS Si concentrations for three Si cell temperatures. The Si concentration is 0.12×10^{18}–1.3×10^{18} cm^{-3} for 1060–1140 °C. Then a series of Si doped GaN samples were grown on undoped GaN templates with seven Si cell temperatures for Hall effect measurements at room temperature. The electron concentrations were extracted by using the two-layer Hall model. The electron concentration of 2.2×10^{18} cm^{-3} is obtained at 1150 °C. When the Si cell temperature reaches 1300 °C, the electron concentration of 1.1×10^{20} cm^{-3} is obtained.

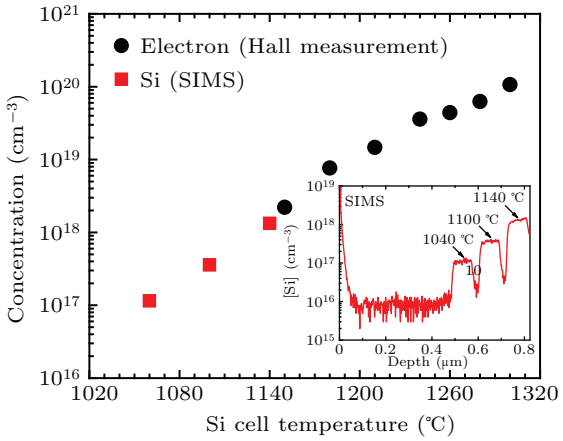


Fig. 9. Si concentration and electron concentration as a function of Si cell temperature. The inset is the Si concentration depth profile measured by SIMS for a stepped Si doped GaN epilayer for three Si cell temperatures.

4. Conclusions

For GaN PA-MBE growth in the optimal window with low growth rates (less than 0.2 μm/h), the growth demonstrates some similarities to that at higher growth rates, but also shows some distinctions. The distinctions are as follows: no 2D layer by layer growth mode has been observed; the Ga flux required to maintain the Ga adlayer (two monolayers) coverage in the growth front is obviously higher than the usual cases; the growth rate shows extremely strong dependence on growth temperatures in the optimal temperature window. For active nitrogen supply varying in a relatively small range, the GaN growth rate increases with increasing flow rate and plasma power, similar to the usual cases. The GaN crystalline quality is mainly determined by the growth temperature and III/V ratio. Similar to MBE grown GaN with usual growth rates, three growth regions, Ga droplets, slightly Ga-rich and 3D growth regions, have been identified across a wide temperature range, from 580 °C to 790 °C. The slightly Ga-rich region is the preferred region, in which the grown GaN epilayers demonstrate optimal crystalline quality, which is characterized with streaky RHEED patterns, smooth surface morphology with clear atomic steps, and very low defect related yellow and blue luminescence bands. Growth temperature is a critical parameter to obtain high quality materials. GaN quality has been greatly improved as the growth temperature increases from below 600 °C to the optimal growth temperature window (∼ 680–760 °C). At extremely high growth temperatures (790 °C), severe GaN decomposition happens, which results in much reduced growth rate. Extremely high Ga flux is required to keep step flow growth mode, which is the consequence of high decomposition rate, low sticking coefficient and exponentially increased desorption rate. Mg and Si dopings of MBE GaN epilayers were grown at the optimal growth temperature and III/V ratio. Mg concentration was controlled by the Mg cell temperature and P type GaN was obtained. Si concentration and electron concentration from 10^{17} cm^{-3} to 10^{20} cm^{-3} in GaN epilayers was obtained by modifying the Si cell temperature.

Acknowledgements

Project supported by the National Natural Science Foundation of China (Grant Nos. 62074077, 61921005, 61974062, and 61974065), the Fundamental Research Funds for the Central Universities, China (Grant No. 14380166), Key R&D Program of Jiangsu Province, China (Grant No. BE2020004-3), the National Key R&D Program of China (Grant No. 2017YFB0404101), Nature Science Foundation of Jiangsu Province, China (Grant No. BE2015111), Collaborative Innovation Center of Solid State Lighting and Energy-saving Electronics.

References

[1] Akasaki I, Amano H and Nakamura S 2014 *R. Swed. Acad. Sci. Nobel Prize Phys.*
[2] Amano H, Baines Y, Beam E, *et al.* 2018 *J. Phys. D: Appl. Phys.* **51** 163001
[3] Zhang Y, Dadgar A and Palacios T 2018 *J. Phys. D: Appl. Phys.* **51** 273001
[4] Khoury M, Li H, Li P, Chow Y C, Bonef B, Zhang H, Wong M S, Pinna S, Song J, Choi J, Speck J S, Nakamura S and DenBaars S P 2020 *Nano Energy* **67** 104236
[5] Zhang H J, Li H J, Li P P, Song J, Speck J S, Nakamura S and DenBaars S P 2020 *ACS Photon.* **7** 1662
[6] Lu W F, Goto N, Murakami H, Sone N, Iida K, Terazawa M, Han, D P, Iwaya M, Tekeuchi T, Kamiyama S and Akasaki I 2020 *Appl. Surf. Sci.* **509** 145271
[7] Ito K, Lu W F, Sone N, Miyamoto Y, Okuda R, Iwaya M, Tekeuchi T, Kamiyama S and Akasaki I 2020 *Nanomaterials* **10** 135
[8] Jorgensen K F, Bonef B and Speck J S 2020 *J. Cryst. Growth.* **546** 125738
[9] Myers D J, Espenlaub A C, Gelzinyte K, Young E C, Martinelli L, Peretti J, Weisbuch C and Speck J S 2020 *Appl. Phys. Lett.* **116** 091102

[10] Li H, Hanus R, Polanco C A, Zeidler A, Koblmüller G, Koh Y K and Lindsay L 2020 *Phys. Rev. B* **102** 014313

[11] Storm D F, Growden T A, Cornuelle E M, Peri P R, Osadchy T, Daulton J W, Zhang W D, Katzer D S, Hardy M T, Nepal N, Molnar R, Brown E R, Berger P R, Smith D J and Meyer D J 2020 *J. Vac. Sci. Technol. B* **38** 032214

[12] Smorchkova I P, Haus E, Heying B, Kozodoy P, Fini P, Ibbetson J P, Keller S, DenBaars S P, Speck J S and Mishra U K 2000 *Appl. Phys. Lett.* **76** 718

[13] Kim K C, Schmidt M C, Sato H, Wu F, Fellows N, Saito M, Fujito K, Speck J S, Nakamura S and DenBaars S P 2007 *Phys. Stat. Sol. (RRL)* **1** 125

[14] Ivanov S V, Nechaev D V, Sitnikova A A, Ratnikov V V, Yagovkina M A, Rzheutskii N V, Lutsenko E V and Jmerik V N 2014 *Semicond. Sci. Technol.* **29** 084008

[15] Zhang H P, Xue J S, Fu Y R, Yang M, Zhang Y C, Duan X L, Qiang W T, Li L X, Sun Z P, Ma X H, Zhang J C and Hao Y 2020 *J. Cryst. Growth* **535** 125539

[16] Poblenz C, Waltereit P and Speck J S 2005 *J. Vac. Sci. Technol. B: Microelectron. Process. Phenom.* **23** 1379

[17] Koblmüller G, Fernández-Garrido S, Calleja E and Speck J S 2007 *Appl. Phys. Lett.* **91** 161904

[18] McSkimming B M, Wu F, Huault T, Chaix C and Speck J S 2014 *J. Cryst. Growth* **386** 168

[19] Gunning B P, Clinton E A, Merola J J, Doolittle W A and Bresnahan R C 2015 *J. Appl. Phys.* **118** 155302

[20] Tarsa E J, Heying B, Wu X H, Fini P, DenBaars S P and Speck J S 1997 *J. Appl. Phys.* **82** 5472

[21] Heying B, Averbeck R, Chen L F, Haus E, Riechert H and Speck J S 2000 *J. Appl. Phys.* **88** 1855

[22] Koblmüller G, Averbeck R, Riechert H and Pongratz P 2004 *Phys. Rev. B* **69** 035325

[23] VanMil B L, Guo H C, Holbert L J, Lee K, Myers T H, Liu T and Korakakis D 2004 *J. Vac. Sci. Technol. B* **22** 2149

[24] Koblmüller G, Brown J, Averbeck R, Riechert H, Pongratz P and Speck J S 2005 *Appl. Phys. Lett.* **86** 041908

[25] Heying B, Tarsa E J, Elsass C R, Fini P, DenBaars S P and Speck J S 1999 *J. Appl. Phys.* **85** 6470

[26] Adelmann C, Brault J, Jalabert D, Gentile P, Mariette H, Mula G and Daudin B 2002 *J. Appl. Phys.* **91** 9638

[27] Tsai J K, Lo I, Chuang K L, Tu L W, Huang J H, Hsieh C H and Hsieh K Y 2004 *J. Appl. Phys.* **95** 460

[28] Zywietz T, Neugebauer J and Scheffler M 1998 *Appl. Phys. Lett.* **73** 487

[29] Neugebauer J, Zywietz T K, Scheffler M, Northrup J E, Chen H and Feenstra R M 2003 *Phys. Rev. Lett.* **90** 056101

[30] Wang X Q and Yoshikawa A 2004 *Prog. Cryst. Growth Charact. Mater.* **48/49** 42

[31] Choi S J, Kim T H, Brown A, Everitt H O, Losurdo M, Bruno G and Moto A 2006 *Appl. Phys. Lett.* **89** 181915

[32] Koblmüller G, Brown J, Averbeck R, Riechert H, Pongratz P and Speck J S 2005 *Jpn. J. Appl. Phys.* **44** L906

[33] Oehler F, Zhu T, Rhode S, Kappers M J, Humphreys C J and Oliver R A 2013 *J. Cryst. Growth* **383** 12

[34] Armitage R, Hong W, Yang Q, Feick H, Gebauer J, Weber E R, Hautakangas S and Saarinen K 2003 *Appl. Phys. Lett.* **82** 3457

[35] Lyons J L, Janotti A and Van de Walle C G 2010 *Appl. Phys. Lett.* **97** 152108

[36] Li S T, Jiang F Y, Fan G H, Wang L, Xiong C B, Peng X X and Mo H L 2004 *J. Lumin.* **106** 219

[37] Demchenko D O, Diallo I C and Reshchikov M A 2016 *J. Appl. Phys.* **119** 035702

[38] Reshchikov M A 2019 *Appl. Phys. Lett.* **115** 262102